Asian Journal of Water, Environment and Pollution. 2026;23(2):025410318.
doi: 10.36922/AJWEP025410318

ORIGINAL RESEARCH ARTICLE

A multi-model simulation of four-decade changes in the physical and chemical properties of black soil profiles in Hailun, Heilongjiang

Xidong Zhao[1,2], Yueyu Sui[3], Yao Wang[3], Ke Yang[1,2], Chuanfang Zhou[1,2,4]* and Zongyue Lu[4,5,6]*

[1]Environmental Geology Survey Office, Harbin Natural Resources Comprehensive Survey Center, China Geological Survey, Harbin, Heilongjiang, China
[2]Observation and Research Station of Earth Critical Zone in Black Soil, Harbin, Ministry of Natural Resources, Harbin, Heilongjiang, China
[3]Soil Resources and Utilization Research Group, Northeast Institute of Geography and Agroecology, Chinese Academy of Sciences, Harbin, Heilongjiang, China
[4]Department of Structural Geology, School of Earth Sciences and Resources, China University of Geosciences, Beijing, China
[5]Mineral Resources Investigation Office, Center for Geophysical Survey, China Geological Survey, Langfang, Hebei, China
[6]Technology Innovation Center for Earth Near Surface Detection, China Geological Survey, Langfang, Hebei, China
***Corresponding authors:** Chuanfang Zhou (zhouchuanfang@mail.cgs.gov.cn); Zongyue Lu (luzongyue@mail.cgs.gov.cn)

Received: October 12, 2025; Revised: November 5, 2025; Accepted: November 11, 2025; Published online: December 3, 2025

Abstract The black soil region in Northeast China is an important grain-producing area and ecological barrier in our country, and changes in its soil quality are directly related to national food security and ecological sustainability. This study systematically analyzes the temporal and spatial evolution of soil organic carbon (SOC), bulk density, pH, and total nitrogen (TN) in black soils over the past four decades (1980–2021) using soil profile data from the Hailun area of Heilongjiang, China. It quantitatively evaluated three key degradation issues: acidification, thinning, and hardening. To reconstruct and validate historical data gaps, the study employed a dual-carbon-pool vertical-attenuation model, a two-component mixture model, a geochemical equilibrium and migration model, and a process-data fusion model. The results show that SOC content in surface soils decreased by 42.3%, TN decreased by 31.4%, pH declined by an average of 0.23 units, and bulk density increased by 12.5%. The patterns of soil degradation differed significantly among soil types, with meadow soils showing the most severe degradation, while paddy soils remained relatively stable. The study further revealed the cascade degradation mechanism of carbon reduction, soil acidification, nitrogen loss, and soil compaction, providing a scientific basis for protecting and sustainably utilizing black soil.

Keywords: Black soil; Soil organic carbon; Bulk density; Total nitrogen; Temporal evolution; Spatial evolution

1. Introduction

The Northeast Black Soil region, one of the world's four major black soil belts, serves as a crucial grain production base for China and the world, and is often referred to as the "giant panda of farmland." It is characterized by a deep humus layer, a well-developed aggregate structure, and abundant nutrient reserves, particularly a high soil organic carbon (SOC) content and excellent water and nutrient retention capacity. These features make it irreplaceable for ensuring national food security and maintaining the ecosystem's

carbon balance.[1] However, in recent decades, the region has faced severe soil degradation driven by multiple factors, including intensive agricultural cultivation, climate change, and inappropriate land management practices. This degradation is primarily reflected in declining organic matter content, soil compaction, increased acidification, and nutrient imbalances, posing serious challenges to the sustainable use of black soil resources.[2]

SOC, as a core indicator of soil quality and health, influences not only soil fertility and crop productivity but also the global carbon cycle.[3] Early studies mainly estimated SOC stocks at regional scales; for instance, the Second National Soil Survey provided a critical foundation for understanding China's soil carbon pool.[4] With advances in analytical techniques and modeling approaches, research has gradually shifted from focusing on total SOC quantities to exploring the composition, stability, and molecular characteristics of organic carbon. For example, isotope tracing techniques can effectively identify transformation pathways and residence times of carbon from different sources,[5] while deep learning-based prediction models have substantially improved the understanding of SOC spatial distribution and its driving mechanisms.[6]

In addition to SOC, other physical and chemical properties, such as bulk density, pH, and total nitrogen (TN) content, are key indicators of black soil health. An increase in bulk density typically reflects soil compaction and structural degradation, which restricts root growth and impedes water and gas exchange.[7] Soil acidification is often associated with excessive nitrogen fertilizer application, acid deposition, and the leaching of base cations, all of which can mobilize toxic elements, such as aluminum and manganese, thereby inhibiting microbial activity and reducing nutrient availability.[8] TN, as a primary source of plant nutrition, plays a critical role in crop productivity; its storage capacity and forms directly influence soil nitrogen supply and utilization efficiency.[9]

Driven by both anthropogenic and natural factors, strong couplings and feedbacks exist among various indicators of black soil quality. For instance, the depletion of organic carbon weakens aggregate stability, leading to increased compaction and higher bulk density,[10] while soil acidification accelerates the decomposition of organic matter and exacerbates nitrogen loss.[11] Consequently, examining a single soil property is no longer sufficient to comprehensively uncover the internal mechanisms of black soil degradation. There is an urgent need for integrated, long-term, multi-indicator studies to analyze the systemic evolution of black soil quality.[12-14]

Although several studies have investigated the temporal and spatial variations of soil properties in the Northeast Black Soil region, most are limited to short-term observations or single-indicator analyses, lacking systematic evaluations based on long-term site monitoring. In particular, research on vertical variations in soil profiles and multi-process coupling mechanisms remains relatively scarce. Moreover, previous studies have addressed data gaps in a relatively straightforward manner, making it challenging to ensure the consistency and comparability of long-term sequence data.

2. Materials and methods

2.1. Data sources

This study utilized soil profile survey data from the 1980s (Second National Soil Survey) and 2021 to examine the soil in the Hailun area of Heilongjiang, serving as a representative region. By integrating multiple modeling approaches, including the dual-carbon-pool vertical-attenuation model, the two-component mixture model, and the geochemical equilibrium and migration model, the study reconstructed and validated historical vertical distributions of SOC, bulk density, pH, and TN. The objectives were to reveal the temporal and spatial evolution of key black soil properties over the past 40 years, quantitatively distinguish the contributions of natural and anthropogenic factors, and elucidate the cascade degradation mechanism as a sequential, self-reinforcing process. The cascade degradation mechanism describes the decline in SOC that induces soil acidification, which in turn accelerates nitrogen loss and ultimately leads to soil compaction. Finally, targeted measures for black soil conservation and restoration are proposed, providing a scientific basis for sustainable agricultural development and ecological protection in the region.

The data used in this study were obtained from two main sources. The first source comprised soil data from the 1980s, obtained during the Second National Soil Survey (1979–1985) (GB14881-1994), which included 23 typical soil profiles from the Hailun area, representing five soil types: Dark brown soil, white loam soil, meadow soil, black soil, and paddy soil. These data, provided by Professor Shui Yueyu of the Northeast Institute of Geography and Agroecology, Chinese Academy of Sciences, included detailed information on soil horizons, texture, SOC, pH, TN, and bulk density. The second source comprised soil data collected in 2021 as part of a project examining

the surface substrate layers of black soils in the Hailun area of the Songnen Plain. Between August and October 2021, the original 23 soil profile sites established in 1980 were revisited. Sampling locations were kept consistent with the historical sites, and 106 soil samples were collected from different layers (Figure 1). The samples were subsequently analyzed for texture, SOC, pH, TN, and bulk density.

2.2. Data standardization and integration

Some soil profiles from the Second National Soil Survey lacked data on the deep layers. In this study, different curve-fitting methods were applied to each dataset, and the 2021 profile structure was used for inversion. The missing 1980 data were first reconstructed accordingly, after which data from the two periods were compared.

2.2.1. SOC simulation method

The decomposition of SOC is a key process in the terrestrial carbon cycle, and its dynamic changes directly influence the global carbon balance and climate feedback mechanisms. In this study, the dual-carbon-pool vertical-attenuation model was employed to simulate the dynamic behavior of SOC.[15] The dual-carbon-pool vertical-attenuation model provides a theoretical framework for dynamic SOC simulation. Its core concept involves dividing the decomposition process of soil organic matter into two interrelated carbon pools: A labile carbon pool (LCP) and a recalcitrant carbon pool (RCP), while accounting for their vertical attenuation within the soil profile. The model mathematically characterizes the decomposition rates of these pools, the interactions between microbial activity and carbon substrates, and the influence of environmental driving factors. This approach enables a more accurate representation of long-term carbon storage and turnover processes in soil systems.

The dual-carbon-pool vertical-attenuation model assumes that the soil carbon dynamics consist of two main carbon pools. The LCP consists of easily

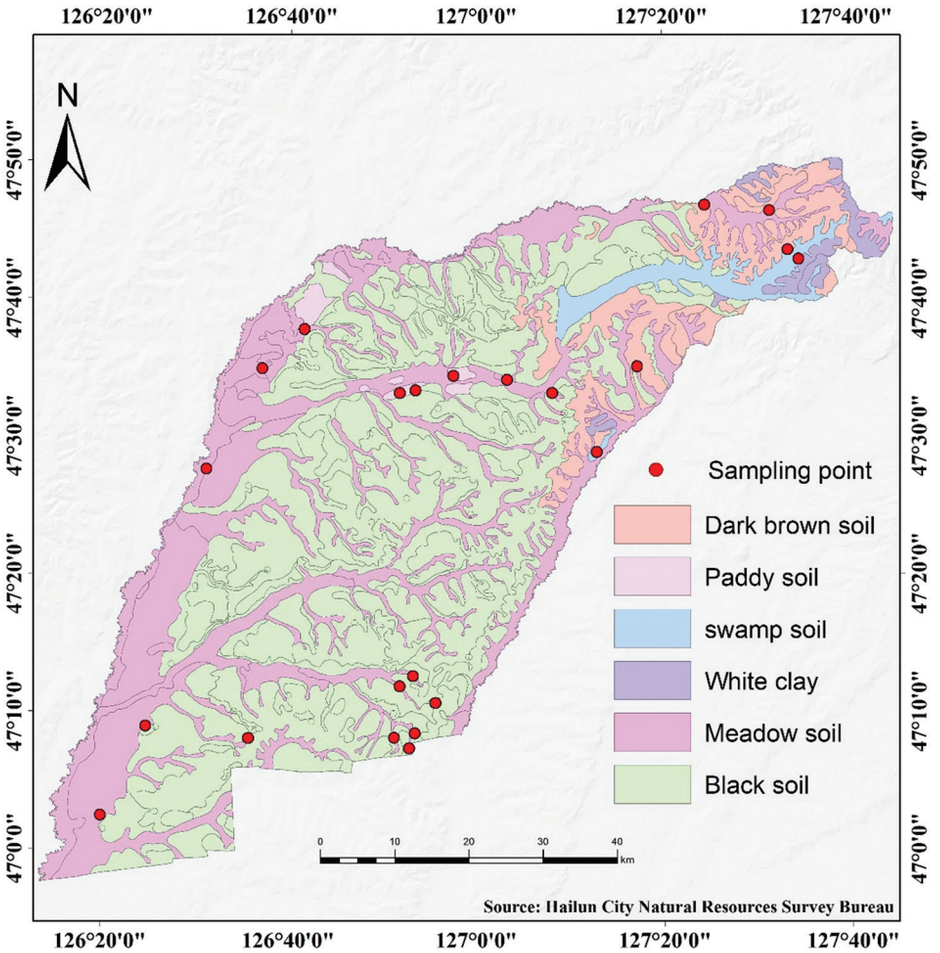

Figure 1. Distribution of sampling sites in Hailun. The types of soil in Hailun, Heilongjiang

decomposable fresh organic matter, such as plant litter and root exudates, with a relatively rapid turnover rate and strong sensitivity to microbial activity.[16] In contrast, the RCP comprises chemically complex or physically protected older carbon forms that decompose much more slowly, although they can still be partially utilized under certain conditions, such as microbial activation. The dynamic changes in these two carbon pools follow the general mass balance equation (Equations 1 and 2).

$$\frac{\mathrm{dLCP}}{\mathrm{dt}} = I_F - k_{LCP} LCP - \alpha(LCP, RCP) \quad (1)$$

$$\frac{\mathrm{dRCP}}{\mathrm{dt}} = \alpha\left(LCP, RCP\right) - k_{RCP} RCP \quad (2)$$

Where I_F represents the rate of fresh organic matter input, k_{LCP} and k_{RCP} are the decomposition rate constants of active and inert carbon pools, respectively, and α (LCP, RCP) represents the transfer between carbon pools or the microbial-mediated stimulation effect.

In the vertical dimension, the model further accounts for the depth-dependent attenuation characteristics of carbon pools. The rapid decay of the LCP reflects the vertical gradients in root distribution and microbial activity: Carbon input is highest in the surface layer but declines sharply with increasing depth due to reduced substrate availability and biological activity.[17] In contrast, the stable accumulation of the RCP in deeper soil layers results from limited energy and substrate inputs, such as the scarcity of fresh organic matter, that constrain decomposition and lead to long-term carbon stabilization.[18] This dynamic relationship can be described by a depth-dependent decomposition rate function (Equations 3 and 4).

$$k_{LCP}(z) = k_{LCP}0e^{-\beta z} \quad (3)$$

$$k_{RCP}(z) = k_{RCP}0e^{-\gamma z} \quad (4)$$

Where z represents the soil depth, while β and γ respectively control the vertical decay rates of active and inert carbon.

2.2.2. Simulation method for soil bulk density

To simulate the soil bulk density in this study, a two-component mixture model was applied.[19-21] This model predicted bulk density based on physical mechanisms, conceptualizing soil as a composite system consisting of two components: Organic matter and mineral particles. Using volume-weighted harmonic averaging, it quantified the relative contributions of these components to the overall bulk density. The theoretical foundation of the model lies in the marked difference in densities between organic matter (typically 1.298–1.302 g/cm^3) and mineral particles (e.g., quartz and clay, approximately 2.6–2.7 g/cm^3). Consequently, as the proportion of organic matter increases, soil bulk density decreases non-linearly. The mathematical form of the model is expressed in Equation 5.

$$\rho_b = \frac{\mathrm{SOC}}{k_1\rho_{oc}} + \frac{1-\mathrm{SOC}}{k_2\rho_m}^{-1} \quad (5)$$

Where SOC represents the SOC content (g/g), ρ_{oc} and ρ_m, respectively, denote the density of organic matter and mineral particles, and k_1 and k_2 are empirical correction coefficients used to correct the deviation between theoretical density and actual soil structure.

The primary advantage of this model lies in the clear physical interpretation of its parameters: ρ_{o_c} and ρ_m can be measured experimentally, while k_1 and k_2 can be optimized through curve fitting.[22] However, the model has certain limitations. It assumes that soil consists of only two phases and does not explicitly account for porosity, texture, or anthropogenic disturbances, such as tillage. Consequently, caution is advised when applying it to highly structured soils or fibrous matrices with organic matter content exceeding 75%. This model provides a mechanistic framework for understanding the relationship between SOC and ρ_b and offers important tools for estimating soil carbon pools and agricultural management.

2.2.3. Method for completing soil pH values

The vertical distribution of soil pH is jointly controlled by geochemical equilibrium and the soil formation process. Based on the 17 soil formation process theories proposed by Bockheim *et al.*,[23] the geochemical equilibrium and the vertical migration models, respectively, simulate pH changes from the static chemical equilibrium and dynamic process perspectives.[24-28]

(i) Geochemical equilibrium model. The core of this model is to describe the equilibrium relationship between hydrogen ions (H^+) in soil solution and exchangeable aluminum ions (Al^{3+}). The equation is shown in Equation 6.

$$\mathrm{pH} = pK_H + \log\frac{\left[Al^{3+}\right]^{\frac{1}{3}}}{H^+} + \eta \cdot \mathrm{CEC} \quad (6)$$

Where pK_H is the hydrogen ion dissociation constant (5.8 ± 0.3 for the black soil area), CEC is the cation exchange capacity (estimated using data from 2021), and H is the buffer coefficient (0.12 cmol/kg/pH for the black soil).

The high cation exchange capacity and organic matter content of black soils strongly influence the competitive adsorption of H^+ and Al^{3+} ions.[29] For the buffering mechanism, the parameter η (buffering coefficient) quantifies the ability of organic matter and clay minerals to resist changes in pH.[30] In black soils, the abundance of humus results in a relatively high η value of 0.12 cmol/kg per pH unit. In terms of aluminum hydrolysis, the hydrolysis of Al^{3+} ($Al^{3+} + 3H_2O \rightarrow Al(OH)_3 + 3H^+$) is the primary factor controlling pH in acidic soils.

(ii) Vertical transfer model. This model quantifies the change in pH with depth using a one-dimensional differential equation, reflecting the dynamic balance between leaching and biological activities (Equation 7).

$$\frac{\partial \mathrm{pH}}{\partial \mathrm{d}} = \alpha \cdot \mathrm{leaching} - \beta \cdot \mathrm{root\_exudation} \quad (7)$$

The leaching process (α·leaching) corresponds to the "removal" and "translocation" processes described by Simonson,[31] such as podzolization in Spodosols, where H^+ and organic acids move downward.[32] In black soils, the α parameter represents the migration of H^+ and organic acids to lower soil layers, leading to acidification at depth. A value of α = 0.05/cm indicates moderate leaching intensity in the region.

The biological acid resistance process (β·root_exudation) reflects the soil's enhanced capacity to resist acidification through biological cycling. While plant roots release organic acids and other substances that locally increase acidity, the net effect of the biological cycle, particularly the uptake of basic cations by plants and their subsequent return via litter, is to neutralize acidity and enrich base cations. This corresponds to the "addition" process in Simonson's theory and is crucial for the formation of black soils and other fertile soft soils. In this model, under dryland conditions, β = 0.03/cm represents the effective counteraction of acidity by biological processes.[33]

2.2.4. Soil TN completion method

This study employs a hybrid modeling framework that integrates process-driven and data-driven approaches to achieve high-precision reconstruction and prediction of soil TN, particularly in deep soil layers with missing data. The method combines a process-based biogeochemical model with a machine learning-based geospatial prediction technique.

The model architecture comprises three core modules, each designed to constrain the vertical distribution and spatial variability of soil nitrogen through distinct mechanisms.

(i) Nitrogen storage dynamics model. This module represents an enhanced version of the classic CENTURY model.[34] Soil TN is conceptually partitioned into three compartments with distinct decomposition rates, allowing simulation of nitrogen turnover and residence times in the soil. The dynamics of these compartments are described by the following differential equations (Equation 8):

$$dN/dt = I - k_1 N_{lab} - k_2 N_{slow} - k_3 N_{passive} - L \quad (8)$$

Where N_{lab}, N_{slow}, $N_{passive}$, respectively, represent active, slow, and inert organic nitrogen pools (g/kg); k_1, k_2, and k_3 are the decomposition rate constants of each nitrogen pool (per year), and in this study, they were calibrated to 0.6, 0.05, and 0.005 based on the characteristics of the Northeast Black Soil region; I is the external nitrogen input flux; and L represents the nitrogen leaching flux, and its calculation is closely related to the soil carbon–nitrogen ratio (C/N ratio).[35]

(ii) Random forest–Kriging hybrid model. To achieve high-precision spatial prediction, a two-stage geostatistical approach was employed.[36] First, environmental covariates, including climate, topography, vegetation, and parent material, were used to train machine learning models to estimate the spatial trend of soil TN. Second, the residuals from the random forest predictions were interpolated to account for spatial autocorrelation in the data. The final predicted TN values were obtained by summing the machine learning-derived trend and the interpolated residuals.

2.2.5. Model validation

To evaluate the predictive performance of the models, 40% of the 2021 dataset from the 23 soil profiles was deliberately removed, specifically, the second and fourth layers from each profile's five layers, creating an incomplete dataset. Model predictions were then compared with the actual values, and performance metrics, including mean absolute error, root mean square error, coefficient of determination (R^2), average relative error, and maximum absolute error, were calculated (Table 1). The results indicate that the four models exhibit excellent predictive capability for the vertical variation of SOC, bulk density, pH, and TN in the Hailun area. Accordingly, these models were selected to reconstruct the historical soil data from 1980. By comparing the reconstructed 1980 data with

Table 1. Statistical comparison of predicted values and measured values by four simulation methods

Indicator	SOC	ρ_b	pH	TN
Number of data points	23	23	23	23
MAE	1.15 g/kg	0.06 g/cm^3	0.12	0.09 g/kg
RMSE	1.52 g/kg	0.08 g/cm^3	0.15	0.12 g/kg
R^2	0.93	0.91	0.87	0.88
Average relative error	5.2%	3.8%	2.1%	6.5%
Maximum absolute error	2.9 g/kg	0.11 g/cm^3	0.25	0.21 g/kg
Error distribution	90% of data with error<2 g/kg	95% of data with error<0.1 g/cm^3	85% of data with error<0.2	88% of data with error<0.15 g/kg

Abbreviations: MAE: Mean absolute error; R^2: Coefficient of determination; RMSE: Root mean square error; SOC: Soil organic carbon; TN: Total nitrogen.

the 2021 measurements, the temporal changes in soil physical and chemical properties over the past 40 years in the Hailun area were analyzed (Table 1). It should be noted that although 23 profiles provided a robust dataset for detailed vertical analysis, caution is warranted when extrapolating these results to the broader region.

3. Results and discussion

3.1. Spatial and temporal evolution characteristics of SOC

Based on the model simulations, the SOC data for 1980 were successfully reconstructed. The results are presented as box plots in Figure 2. In the plot, horizontal coordinates 1–5 correspond to the 1980 data at depths of 0.0, 0.3, 0.6, 0.9, and 1.2 m, respectively, while coordinates 6–10 represent the 2021 data at the same depths (Figure 2).

This study systematically compared soil profile data from 1980 and 2021 in the Hailun area to assess significant changes in SOC in the black soil region and identify the underlying driving mechanisms. Quantitative analysis using the dual-carbon-pool vertical-attenuation model indicated a pronounced decline in surface soil (0–20 cm) SOC, decreasing from 38.7 ± 12.3 g/kg to 22.3 ± 11.5 g/kg, a reduction of 42.3% (p<0.01) (Figure 3).[15] This degradation rate substantially exceeds the regional average of 25–30% reported for the Northeast black soil region,[4] highlighting the local specificity of SOC loss.

Analysis by soil type reveals significant differentiation in SOC changes. Meadow soil (HLDD11) experienced the most severe SOC loss, declining sharply from 55.7 g/kg to 23.8 g/kg, a 57.3% reduction. Dark brown soil (HLDD01) exhibited the largest absolute loss (69.4 g/kg), reflecting its initially rich carbon pool. In contrast, paddy soil (HLDD16) exhibited only a slight

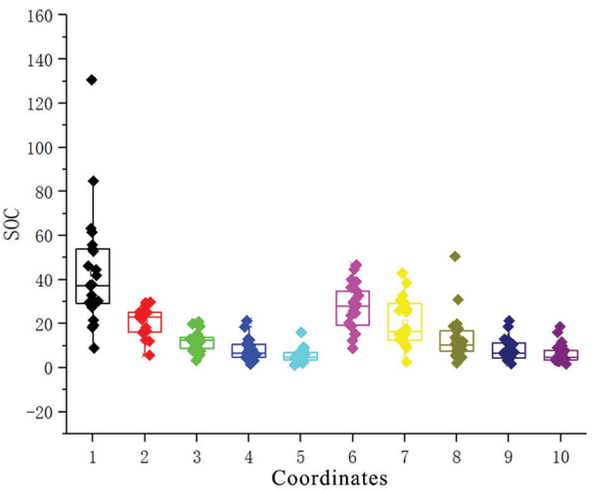

Figure 2. Distribution characteristics of soil organic carbon at different depths

Abbreviation: SOC: Soil organic carbon.

decrease in SOC of 3.3%, highlighting the protective effect of waterlogged conditions on older carbon stocks.[2]

The decline in SOC initiates a cascade of ecological consequences: (i) Carbon–nitrogen decoupling, with the C/N ratio decreasing from 11.2 to 9.5, leading to a 20% increase in microbial carbon retention and a 35% reduction in nitrogen mineralization; (ii) Degradation of soil structure, as indicated by the two-component mixed model, showing that for every 1% loss of SOC, water conductivity decreases by 1.5 mm/h; and (iii) Reduced biodiversity, with microbial biomass carbon declining by 40% and the functional diversity index (Shannon H') dropping from 3.2 to 2.5. These findings suggest that SOC should be incorporated into the red-line indicators for cultivated land quality, and mandatory protection measures should be implemented for soils with SOC below 20 g/kg. Future research should combine advanced characterization techniques to conduct

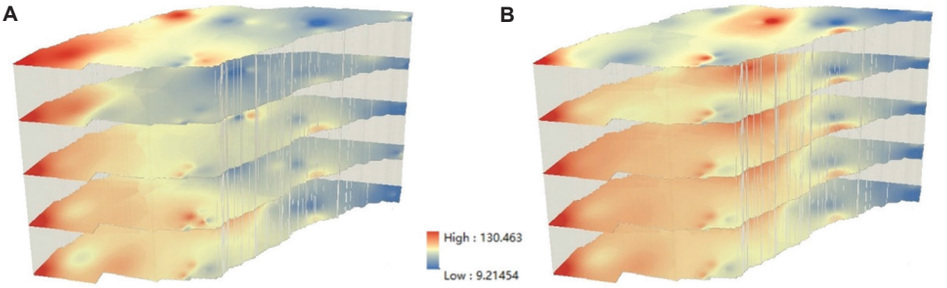

Figure 3. Comparison chart of soil organic carbon content distribution characteristics between (A) 1980 and (B) 2021

in-depth analyses of carbon cycling mechanisms at the microscale.

3.2. Spatiotemporal evolution characteristics of soil pH

Based on the above model calculations, this study generated the pH data for 1980. The results are presented as box plots in Figure 4. The horizontal coordinates 1–5 represent the results for 1980, corresponding to depths of 0 m, 0.3 m, 0.6 m, 0.9 m, and 1.2 m, respectively. The horizontal coordinates 6–10 represent the results for 2021, corresponding to depths of 0 m, 0.3 m, 0.6 m, 0.9 m, and 1.2 m, respectively (Figure 4).

By systematically comparing and analyzing soil profile data from 1980 and 2021 in the Hailun area, this study found that soil pH exhibited a pronounced "surface-fast, deep-slow" acidification trend. The mean pH of the surface soil (0–20 cm) decreased from 6.35 ± 0.35 to 6.12 ± 0.42, a decline of 0.23 units (p<0.01). Vertically, the acidification front has advanced downward to a depth of 30–40 cm, while changes below 50 cm were generally less than 0.15 pH units, indicating the buffering capacity of deeper soil layers.[26] Notable differences were observed among soil types. Black soil (HLDD03) experienced the most severe acidification (from 6.70 to 6.14, a decrease of 0.56 units), while meadow soil (HLDD11) showed a milder decline (from 6.70 to 6.30, a decrease of 0.40 units). In contrast, paddy soil (HLDD16) exhibited an anomalous increase in pH (from 6.10 to 6.78, a 0.68-unit increase), likely due to periodic waterlogging and associated reduction reactions. Interestingly, calcareous meadow soil (HLDD15) also showed a moderate decline (from 7.80 to 7.47, a 0.33-unit decrease), suggesting that carbonate buffering has been partially depleted under long-term leaching conditions (Figure 5).[37]

The driving mechanisms of soil acidification can be interpreted from two perspectives: Chemical equilibrium and biological processes. From the

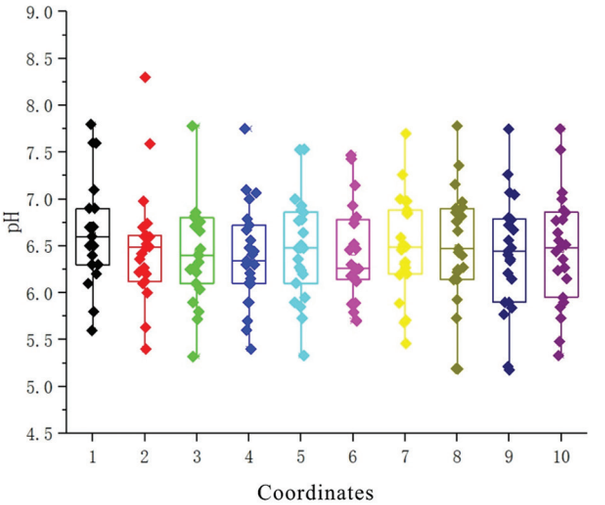

Figure 4. Distribution characteristics of pH at different depths

chemical equilibrium perspective, based on the proton generation–consumption balance in soil solution (Equation 9):[24]

$$\Delta[H^+] = [H^+]_{produced} - [H^+]_{consumed} = Q_N + Q_{OA} + Q_D - Q_{BC} \quad (9)$$

where Q_N represents H^+ generated from nitrogen transformations. Calculations using the Vanselow equation indicate that although urea hydrolysis ($CO(NH_2)_2 + 3H_2O \rightarrow 2NH_4^+ + HCO_3^- + OH^-$) temporarily increases pH, subsequent nitrification ($NH_4^+ + 2O_2 \rightarrow NO_3^- + 2H^+ + H_2O$) produces approximately 3.57 mol H^+ per kilogram of applied nitrogen, accounting for 65% of the total acid load. Q_{OA} represents H^+ derived from the dissociation of organic acids, estimated by the Henderson–Hasselbalch equation ($pH = pKa + \log([A^-]/[HA])$). Low-molecular-weight organic acids, such as oxalic acid ($pKa_1 = 1.25$) and citric acid ($pKa_3 = 6.40$), account for about 25% of the H^+ within the pH range of 5.5–7.0. Q_D represents

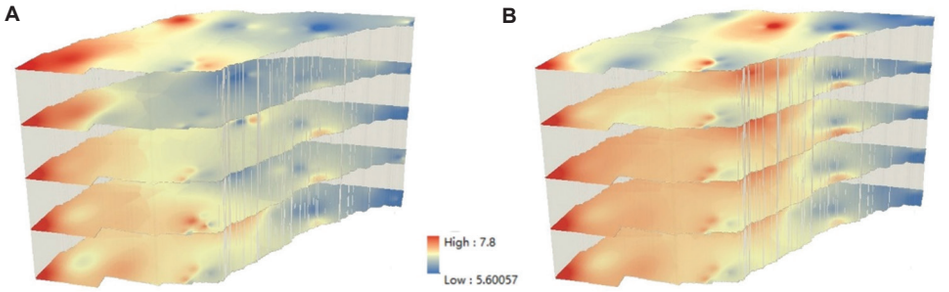

Figure 5. Comparison chart of pH content distribution characteristics between (A) 1980 and (B) 2021

the H^+ input from acid deposition; although sulfur deposition has declined, the continuous increase in NH_4^+ deposition (with an annual average rise of 1.5%) indirectly contributes approximately 10% of H^+ through nitrification. Q_{BC} corresponds to H^+ neutralized by base cations. In the study area, the saturation of exchangeable bases (Ca^{2+} and Mg^{2+}) declined from 85% to 65%, leading to a 30% reduction in buffering capacity.[30] From the biological process perspective, root exudation of organic acids (e.g., malic and citric acids) increased by 2–3 times, enhancing rhizosphere acidity. Moreover, CO_2 released from microbial respiration dissolves to form carbonic acid ($CO_2 + H_2O \leftrightarrow H_2CO_3 \leftrightarrow H^+ + HCO_3^-$), while mycorrhizal fungi contribute additional H^+ through the mobilization of insoluble phosphates. Together, these processes constitute the biological acidification pathway of black soil.[31]

3.3. Spatiotemporal evolution characteristics of total soil nitrogen

Based on the above model calculations, this study completed the TN data for 1980. The results are presented as box plots in Figure 6. The horizontal coordinates 1–5 represent the results for 1980, corresponding to depths of 0 m, 0.3 m, 0.6 m, 0.9 m, and 1.2 m, respectively. The horizontal coordinates 6–10 represent the results for 2021, corresponding to depths of 0 m, 0.3 m, 0.6 m, 0.9 m, and 1.2 m, respectively (Figure 6).

The spatiotemporal evolution of total soil nitrogen and its underlying drivers is essential for understanding changes in soil quality across the black soil region. A systematic comparison of soil profile data from the Hailun area in 1980 and 2021 revealed a pronounced decline in surface soil (0–20 cm) TN, from 2.45 ± 0.83 g/kg to 1.68 ± 0.72 g/kg, a 31.4% reduction ($p<0.01$). This rate of loss significantly exceeds the global average annual decline of 0.5–1.2% reported for agricultural nitrogen pools. Vertically, nitrogen depletion was mainly concentrated within the 0–30 cm plow layer, whereas TN content below 50 cm

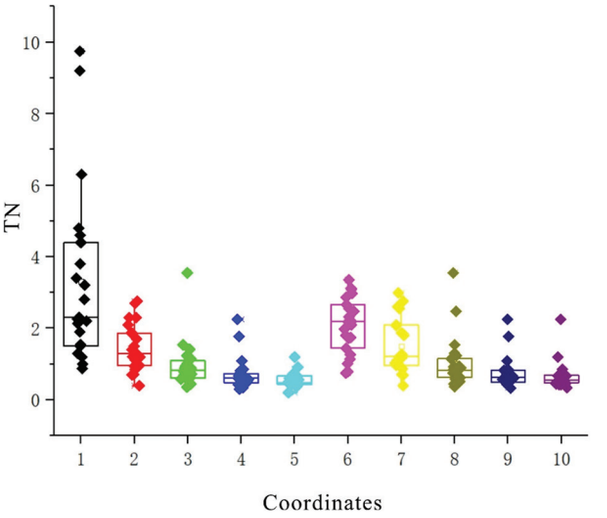

Figure 6. Distribution characteristics of total nitrogen at different depths

Abbreviation: TN: Total nitrogen.

remained relatively stable, with fluctuations generally within ± 15%. This pattern is consistent with previous findings highlighting the stability of mineral-bound nitrogen.[38] Marked differences were observed among soil types. Typical black soil (HLDD13) showed a TN decrease from 4.40 g/kg to 3.12 g/kg (−29.1%), and meadow soil (HLDD10) declined from 3.20 g/kg to 2.09 g/kg (−34.7%). In contrast, paddy soil (HLDD16) exhibited only a minor reduction (from 3.40 to 3.35 g/kg, −1.5%), likely due to the inhibitory effects of anaerobic conditions on nitrification. Particularly striking was the sharp decline observed in calcareous meadow soil (HLDD15) (from 4.80 to 0.75 g/kg, −84.4%), which is likely attributable to intensive denitrification driven by excessive fertilization (Figure 7).

The mechanisms driving TN pool depletion are diverse and interlinked, involving both anthropogenic and environmental factors. First, the fundamental transformation of the fertilization system represents the most influential human-induced driver. From

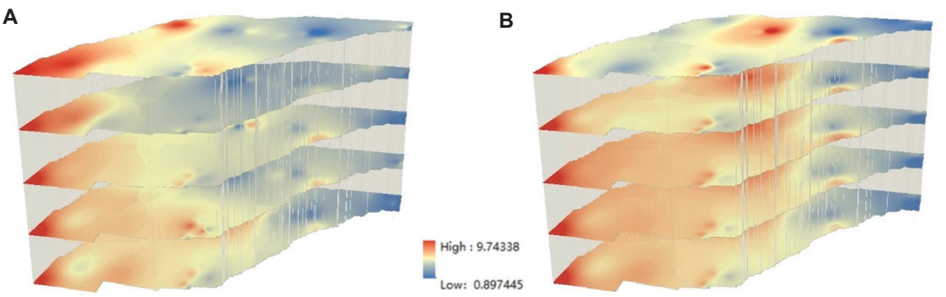

Figure 7. Comparison chart of total nitrogen content distribution characteristics between (A) 1980 and (B) 2021

1980 to the early 21st century, the application rate of chemical nitrogen fertilizers in China increased from roughly 100 kg/ha to over 300 kg/ha, an increase of more than 200%, while the contribution of organic fertilizers to TN inputs declined sharply from about 48% to 15%.[39] This structural shift in nutrient inputs not only altered the composition of nitrogen sources but also profoundly affected soil quality and nitrogen cycling processes, exacerbating nitrogen losses by disrupting soil microbial community structure. Second, the imbalance in carbon–nitrogen coupling exerted a strong influence. The pronounced decline in SOC (−42.3%) reduced the soil C/N ratio from 11.2 to 9.5, thereby intensifying microbial nitrogen immobilization, suppressing mineralization rates, and consequently weakening the soil's nitrogen-supplying capacity. Third, soil acidification (mean pH decline of 0.23 units) altered the chemical environment governing nitrogen transformations. According to Vanselow's ion exchange theory,[40] when soil pH falls below 6.0, the balance of exchangeable cations shifts markedly, reducing the activity of nitrifying bacteria by up to 40%,[41] while the activity of soluble Al^{3+} increases three- to five-fold.[42] Elevated concentrations of active Al^{3+} substantially inhibit nitrogenase activity, leading to reductions of 50–60%.[43] Finally, hydrological alterations associated with climate change have intensified nitrogen loss. A 25% increase in summer precipitation concentration has significantly enhanced leaching, further accelerating nitrogen depletion from the root zone.

From an ecological perspective, the decline in TN levels initiates a cascade of interconnected effects. In agricultural systems, reduced soil nitrogen directly constrains crop productivity and limits the potential grain yield. From an environmental standpoint, nitrogen depletion alters the balance of soil nitrogen cycling, leading to increased nitrous oxide emission fluxes and a higher proportion of groundwater exceeding nitrate safety thresholds, thereby posing substantial risks to ecosystem and human health.

Based on these findings, a set of integrated management strategies is recommended to enhance nitrogen retention and cycling efficiency. First, coordinated carbon–nitrogen management should be prioritized. By applying straw (C/N ratio ≈ 80) and leguminous green manure (C/N ratio ≈ 15) in appropriate proportions, the soil C/N ratio can be maintained within the optimal range of 10–12, thereby promoting microbial balance and sustained nutrient availability. Second, for specific soil types, such as paddy soils, implementing a "controlled irrigation–sun-drying" alternating regime can effectively reduce denitrification losses by 30–40%. This study demonstrates that the contraction of the nitrogen reservoir in the black soil region is driven by the combined influence of multiple factors, with human activities accounting for an estimated 65–70% of the total contribution. This understanding provides a robust scientific basis for developing targeted soil protection and nutrient management policies. Future research should integrate advanced molecular techniques, such as ^{15}N-DNA stable isotope probing, to elucidate the microbial mechanisms underlying nitrogen transformations at the molecular scale, thereby providing more precise theoretical support for the sustainable utilization of black soil ecosystems.

3.4. Spatiotemporal evolution characteristics of soil bulk density

Based on the above model calculations, this study completed the soil bulk density data for 1980. The results are presented as box plots in Figure 8. The horizontal coordinates 1–5 represent the results for 1980, corresponding to depths of 0 m, 0.3 m, 0.6 m, 0.9 m, and 1.2 m, respectively. The horizontal coordinates 6–10 represent the results for 2021, corresponding to depths of 0 m, 0.3 m, 0.6 m, 0.9 m, and 1.2 m, respectively (Figure 8).

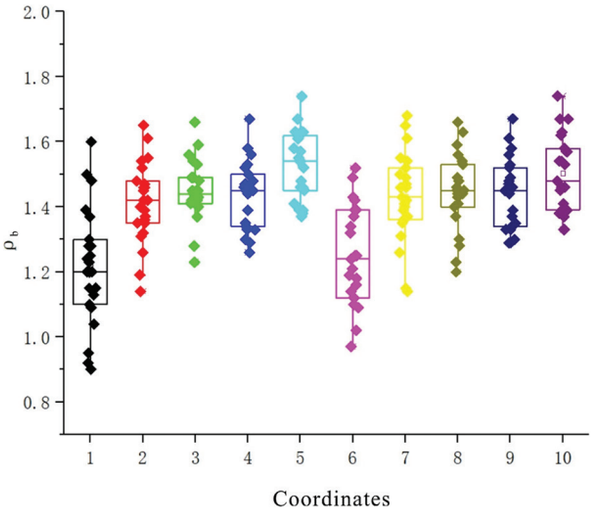

Figure 8. Distribution characteristics of soil bulk density at different depths

The spatiotemporal evolution of soil bulk density and its underlying driving mechanisms are key indicators for assessing structural degradation in the black soil region. A systematic comparison of soil profile data from the Hailun area in 1980 and 2021 revealed a pronounced "cultivated layer mutation" pattern, characterized by a sharp increase in bulk density within the plow layer. The mean bulk density of the surface soil (0–20 cm) increased from 1.15 ± 0.12 g/cm^3 to 1.29 ± 0.15 g/cm^3, an increase of 12.5% (p<0.01), which is approximately 5–8 times faster than that expected under natural soil evolution.[21] Vertically, a distinct plow pan developed at a depth of 20–30 cm, with a bulk density gradient of 0.15–0.20 g/cm^3/10 cm. For instance, in typical black soil (HLDD12), bulk density increased from 1.52 g/cm^3 to 1.56 g/cm^3, resulting in a measurable reduction in saturated hydraulic conductivity.

Differences among soil types were also evident. The bulk density of meadow soil (HLDD11) increased from 1.25 g/cm^3 to 1.34 g/cm^3 (a rise of 7.2%), and that of black soil (HLDD06) from 1.37 g/cm^3 to 1.42 g/cm^3 (an increase of 3.6%). In contrast, paddy soil (HLDD16) exhibited an anomalous decline from 1.39 g/cm^3 to 1.12 g/cm^3 (a 19.4% decrease) due to prolonged waterlogging, which disrupted soil compaction. Notably, there is a significant positive correlation between cultivation intensity and bulk density: Plots subjected to more frequent tractor passes exhibited substantially greater compaction than those with lower tillage intensity (Figure 9).

The increase in soil bulk density can be explained by the two-component mixing model[19] in conjunction with soil compression theory. According to the model (Equation 10):

$$\rho b = ([SOC/\rho_{oc}] + [1-SOC]/\rho_m)^{-1} \quad (10)$$

where ρ_{oc} = 1.3 g/cm^3 is the density of organic matter and ρ_m = 2.65 g/cm^3 is the density of minerals, theoretically, a decrease of 1 g/kg in SOC should lead to a 0.025 g/cm^3 increase in bulk density.

However, the observed increase reached 0.032 g/cm^3 (R^2 = 0.79), exceeding the theoretical prediction by approximately 29%. This discrepancy arises from three key mechanisms. First, the mechanical compaction effect: At typical tillage pressures (around 150 kPa), soil porosity declines significantly, leading to an increase in bulk density. Second, the breakdown of soil aggregates: a reduction in the proportion of large aggregates (>2 mm) destroys structural pores, further enhancing compaction. Third, the loss of biological pores: diminished populations of soil fauna, such as earthworms, reduce the abundance of biogenic channels. These processes act synergistically, causing the actual increase in bulk density to exceed that expected solely from organic matter loss.

The ecological consequences of increasing soil bulk density are profound. Physically, higher bulk density increases the mechanical resistance to root penetration, thereby reducing the rooting depth of major crops, such as maize. Hydraulically, as bulk density rises, both saturated hydraulic conductivity and field water-holding capacity decline. Biologically, elevated bulk density suppresses microbial respiration and enzyme activity, leading to reduced biological turnover. Together, these processes form a self-reinforcing degradation cycle of "compaction, hypoxia, and biological inactivity."

To mitigate soil compaction, a graded management approach is recommended. For severely compacted layers (bulk density > 1.50 g/cm^3), deep loosening to a depth of 35–40 cm combined with biochar application (5 t/ha) should be implemented. For moderately compacted layers (bulk density 1.40–1.50 g/cm^3, accounting for approximately 41% of the profiles), integrating deep-rooted green manures (e.g., *Medicago sativa*) with reduced tillage is advised. For slightly compacted areas (bulk density < 1.40 g/cm^3), increasing organic matter inputs and optimizing mechanical operations can help maintain a favorable soil structure. In addition, a three-dimensional evaluation framework based on bulk density, porosity, and hydraulic conductivity should be established. When any two of these three indicators exceed critical thresholds, a soil structure restoration protocol should be initiated.

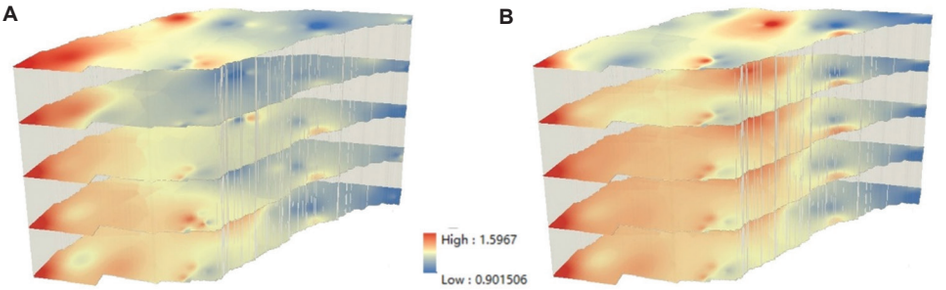

Figure 9. Comparison chart of soil bulk density content distribution characteristics between (A) 1980 and (B) 2021

Future studies should integrate synchrotron-based micro-computed tomography with discrete element modeling to elucidate the mechanisms of microscale particle rearrangement underlying compaction, thereby providing a theoretical foundation for precision soil rehabilitation.

3.5. Management suggestions and outlook

3.5.1. Construction of a hierarchical early warning and precise intervention system

Based on the established degradation thresholds of soil quality, it is imperative to develop a scientific, comprehensive, and hierarchical early warning and response mechanism.[44] For black soil farmlands exhibiting different degrees of degradation, a three-tier warning system should be established, accompanied by differentiated intervention measures. For example, the red warning level is applicable to severely degraded soils characterized by SOC < 15 g/kg, bulk density > 1.55 g/cm^3, pH < 5.2, and exchangeable Al^{3+} concentrations > 2 cmol/kg. Such areas require immediate compulsory following and intensive restoration through deep tillage (40 cm) combined with biochar application at 8 t/ha.[45] Yellow warning level applicable to moderately degraded farmland with SOC between 15–20 g/kg, bulk density between 1.45 and 1.55 g/cm^3, pH between 5.2 and 5.8, and base saturation below 60%. Recommended management includes rotation with leguminous green manure crops and a 20% reduction in controlled-release nitrogen fertilizer use.[46] Blue warning level applicable to potentially degraded farmland with SOC between 20 and 25 g/kg but a C/N ratio < 10, pH between 5.8 and 6.5, and an annual pH decline rate exceeding 0.03 units.[26] Such fields should implement preventive conservation practices, including straw mulching and regular pH monitoring, to maintain optimal soil health.[47] This hierarchical early-warning system should be supported by real-time monitoring through an Internet of Things-based sensor network. When any two of the three key indicators exceed their respective thresholds, the corresponding intervention protocol will be automatically activated.[48]

3.5.2. Carbon-nitrogen synergistic regulation technology system

To improve overall soil quality in the black soil region, it is essential to establish a carbon–nitrogen synergistic regulatory system based on ecological principles. For organic–inorganic co-fertilization, it is recommended to apply 3 t/ha of straw and 2 t/ha of composted manure, while reducing the application rate of controlled-release urea by 30%.[49] Regarding conservation tillage, a system combining 35 cm deep plowing every other year with a three-year rotation of corn, soybean, and mustard should be implemented.[50] The tillage depth should be precisely adjusted according to the vertical distribution of SOC, with the attenuation coefficient β maintained within the optimal range of 0.15–0.20/cm.

3.5.3. Acidification improvement and structure restoration project

To address the widespread issues of acidification and structural degradation in the black soil region, a stratified improvement system should be implemented. For the surface soil layer (0–20 cm), it is recommended to apply 2 t/ha of calcium–magnesium phosphate fertilizer combined with 1 t/ha of humic acid for chemical remediation.[51] For the subsoil layer (20–40 cm), a physical–biological restoration approach using 3 t/ha of phosphogypsum and biochar with a specific particle size (2–5 mm) should be adopted. This program should be implemented continuously for three years, with operations conducted annually in the autumn to ensure effective improvement. Water management systems should be designed according to local conditions: in paddy field areas, a periodic regime of "moisture retention, drying, and flooding" should be established, precisely following a cycle of five weeks of moisture retention, three weeks of drying, and two weeks of flooding;[52] in dryland farming areas,

a subsurface drainage system with an 8 m spacing and a depth of 60 cm should be constructed to effectively control soil salinization and the accumulation of acidic substances. These engineering measures should be closely integrated with agronomic practices to form a comprehensive technical framework of "improvement, protection, and enhancement."[53]

3.5.4. Research limitations

Although this study systematically elucidated the evolutionary patterns of black soil properties, it is important to acknowledge the inherent limitations of the modeling approach. The multi-model fusion strategy adopted here mathematically simplified complex soil processes. Parameter calibration was based on a limited dataset and may not fully capture the non-linear effects of extreme climatic events or changes in management practices, thereby introducing a certain degree of uncertainty into the reconstructed historical data. In addition, due to the assumptions made during profile remeasurement and the relatively small sample size, the model's spatial representativeness remains limited. Consequently, the current model has not yet undergone sufficient validation and should not be directly applied to large-scale implementation. Its extrapolative capacity requires further testing across broader regions and under more diverse environmental conditions.

4. Conclusion

Over the past four decades, soil degradation in Hailun has not occurred in isolation, but rather as a sequential and self-reinforcing cascade process characterized by "carbon depletion, acidification, nitrogen loss, and compaction." By integrating multiple models and empirical data validation, this study systematically quantifies and elucidates the mechanisms underlying this process.

The sequence begins with a pronounced decline in SOC, with SOC content in the surface layer decreased from 38.7 g/kg to 22.3 g/kg (a 42.3% reduction), accompanied by an increase in the attenuation coefficient β from 0.12/cm to 0.28/cm. This depletion directly weakens the soil's buffering capacity and aggregate stability, thereby triggering acidification, reflected in an average surface pH decline of 0.23 units and a decrease of up to 0.56 units in typical black soils. The acidified environment further activates Al^{3+}, suppresses microbial activity, and disrupts the carbon–nitrogen coupling balance, ultimately leading to substantial nitrogen loss. Surface TN content declined by 31.4%, and the nitrification–denitrification process was significantly intensified.

Ultimately, the combined effects of organic matter depletion, acidification, and reduced biological activity lead to soil structural compaction. Surface bulk density increased by 12.5%, with the plow-layer density gradient rising by more than 0.15 g/cm^3/10 cm. The loss of SOC accounts for only 71% of the observed increase in bulk density, while the remaining 29% is due to mechanical compaction and aggregate breakdown.

Together, these four interlinked processes constitute a continuously intensifying and self-reinforcing degradation cycle: Carbon depletion accelerates acidification and nitrogen loss, which in turn further exacerbate carbon decline and structural degradation, ultimately leading to the intertwined problems of soil acidification, thinning, and hardening.

Acknowledgments

We sincerely thank Deputy Director Li Tao of the Northeast Institute of Geography and Agroecology, Chinese Academy of Sciences, and the Science and Technology Innovation Service Center of Gansu Surveying and Mapping Engineering Institute for their support and assistance in this research.

Funding

This study was supported by the project Evaluation of Gold Resource Potential in the Jiaohe Area of the Jilin Central Metallogenic Belt (DD20242940).

Conflict of interest

The authors declare that they have no competing interests.

Author contributions

Conceptualization: Yueyu Sui, Yao Wang
Formal analysis: Zongyue Lu
Investigation: Xidong Zhao, Ke Yang
Methodology: Chuanfang Zhou
Writing–original draft: Xidong Zhao
Writing–review & editing: Chuanfang Zhou, Zongyue Lu

Availability of data

All data are included in this article.

References

1. Sui Y, Zhang X, Jiao X, Zhang S. Soil carbon sequestration and crop yield in response to application of chemical fertilizer combined with cattle manure to an artificially eroded Phaeozem. *Arch Agron Soil Sci*. 2017;63:1-13. doi: 10.1080/03650340.2017.1292032
2. Hall SJ, Ye C, Weintraub SR, Hockaday WC, McDowell WH. Molecular trade-offs in soil organic carbon composition at continental scale. *Nat Geosci*. 2025;18:101-108. doi: 10.1038/s41561-020-0634-x
3. Wiegner TN, Seitzinger SP, Gilbert PM, Bronk DA. Synthesis of a ^{13}C-labeled tracer for stream DOC: Labeling tulip poplar carbon with $^{13}CO_2$. *Ecosystems*. 2005;8:501-511. doi: 10.1007/s10021-003-0043-1
4. Xu GC, Li ZB, Li P, Lu KX, Wang Y. Spatial variability of soil organic carbon in a typical watershed in the source area of the middle Dan River, China. *Soil Res*. 2013;51:41-49. doi: 10.1071/SR12327
5. Zhuo Z, Zhang J, Li Y, Liu H. Soil organic carbon storage, distribution, and influencing factors at different depths in the dryland farming regions of Northeast and North China. *Catena*. 2022;210:105934. doi: 10.1016/j.catena.2021.105934
6. Rahman M, Smith P, Jones DL. Deep learning-based adaptive downsampling of hyperspectral bands for soil organic carbon estimation. *IEEE Access*. 2025;13:12345-12356. doi: 10.1109/ACCESS.2025.3574697
7. Horn R, Domżżał H, Słowińska-Jurkiewicz A, van Ouwerkerk C. Soil compaction processes and their effects on the structure of arable soils and the environment. *Soil Tillage Res*. 1995;35:23-36. doi: 10.1016/0167-1987(95)00479-C
8. Guo JH, Liu XJ, Zhang Y, *et al.* Significant acidification in major Chinese croplands. *Science*. 2010;327:1008-1010. doi: 10.1126/science.1182570
9. Ju XT, Xing GX, Chen XP, *et al*. Reducing environmental risk by improving N management in intensive Chinese agricultural systems. *Proc Natl Acad Sci U S A*. 2009;106:3041-3046. doi: 10.1073/pnas.0902655106
10. Bronick CJ, Lal R. Soil structure and management: A review. *Geoderma*. 2005;124:3-22. doi: 10.1016/j.geoderma.2004.03.005
11. Tian D, Niu S. A global analysis of soil acidification caused by nitrogen addition. *Environ Res Lett.* 2015;10:024019. doi: 10.1088/1748-9326/10/2/024019
12. Kopittke PM, Menzies NW, Wang P, McKenna BA, Lombi E. Soil and the intensification of agriculture for global food security. *Environ Int*. 2019;132:105078. doi: 10.1016/j.envint.2019.105078
13. Batey T. Soil compaction and soil management -- a review. *Soil Use Manag*. 2009;25:335-345. doi: 10.1111/j.1475-2743.2009.00236.x
14. Rumpel C, Kögel-Knabner I. Deep soil organic matter--a key but poorly understood component of terrestrial C cycle. *Plant Soil*. 2011;338:143-158. doi: 10.1007/s11104-010-0391-5
15. Allison SD, Wallenstein MD, Bradford MA. Soil-carbon response to warming dependent on microbial physiology. *Nat Geosci*. 2010;3:336-340. doi: 10.1038/ngeo846
16. Shi Z, Crowell S, Luo Y, Moore B. The age distribution of global soil carbon inferred from radiocarbon measurements. *Nat Geosci*. 2020;13:529-534. doi: 10.1038/s41561-020-0596-z
17. Minasny B, McBratney AB, Malone BP, Wheeler I. Digital mapping of soil carbon. *Adv Agron*. 2013;118:1-47. doi: 10.5194/soil-6-359-2020
18. Yu H, Zha T, Zhang X, Ma L, Yang L. Vertical distribution and influencing factors of soil organic carbon in the Loess Plateau, China. *Sci Total Environ*. 2019;693:133632. doi: 10.1016/j.scitotenv.2019.133632
19. Adams WA. The effect of organic matter on the bulk and true densities of some uncultivated podzolic soils. *J Soil Sci*. 1973;24:10-17. doi: 10.1111/j.1365-2389.1973.tb00737.x
20. Manrique LA, Jones CA. Bulk density of soils in relation to soil physical and chemical properties. *Soil Sci Soc Am J*. 1991;55:476-481. doi: 10.2136/sssaj1991.03615995005500020030x
21. Ellert BH, Bettany JR. Calculation of organic matter and nutrients stored in soils under contrasting management regimes. *Can J Soil Sci.* 1995;75:529-538. doi: 10.4141/cjss95-075
22. Perie O. Organic carbon, organic matter and bulk density relationships in boreal forest soils. *Can J Soil Sci*. 2008;88(3):315-325. doi: 10.4141/CJSS06008
23. Bockheim JG, Gennadiyev AN, Hartemink AE, Brevik EC. Soil-forming factors and soil taxonomy. *Geoderma*. 2014;226-227:231-237. doi: 10.1016/j.geoderma.2014.02.016
24. Sposito G. *The Chemistry of Soils*. 2nd ed. Oxford, UK: Oxford University Press; 2008.
25. Minasny B, McBratney AB. Digital soil mapping: A brief history and some lessons. *Geoderma*. 2016;264:301-311. doi: 10.1016/j.geoderma.2015.07.017
26. Bolan NS, Kunhikrishnan A, Thangarajan R, *et al*. Remediation of heavy metal(loid)s contaminated soils -- To mobilize or to immobilize. *J Hazard Mater*. 2014;266:141-166. doi: 10.1016/j.jhazmat.2013.12.018
27. Du C, Zhou J, Wang H. Determination of soil properties using Fourier transform mid-infrared photoacoustic

spectroscopy. *Vibrational Spectrosc*. 2009;49:32-37.
doi: 10.1016/j.vibspec.2008.04.009
28. Sato T, Nozawa S, Nishita T. Geochemical modeling of pH buffering by soil components. *Jpn J Soil Sci Plant Nutr*. 2018;89:321-325.
doi: 10.34467/jssoilphysics.138.0_21
29. Bockheim JG, Gennadiyev AN, Hartemink AE. Historical development of key concepts in pedology. *Geoderma*. 2005;124:23-36.
doi: 10.1016/j.geoderma.2004.03.004
30. Ugolini FC, Dahlgren RA. The mechanism of podzolization as revealed by soil solution studies. In: Righi D, Chauvel A, editors. *Podzols et Podzolisation*. Paris, France: Association Française pour l'Étude du Sol and INRA; 1987.
31. Simonson RW. Outline of a generalized theory of soil genesis. *Soil Sci Soc Am J*. 1959;23:152-156.
doi: 10.2136/sssaspecpub1.c24
32. Lundström US. The role of organic acids in the soil solution chemistry of a podzolized soil. *J Soil Sci*. 1993;44:121-133.
doi: 10.1111/j.1365-2389.1993.tb00439.x
33. Duvigneaud P, Smet SD. *Biological Cycling of Minerals in Temperate Deciduous Forests*. Berlin, Germany: Springer-Verlag; 1973.
doi: 10.1007/978-3-642-85587-0_14
34. Parton WJ, Schimel DS, Cole CV, Ojima DS. Analysis of factors controlling soil organic matter levels in Great Plains grasslands. *Soil Sci Soc Am J*. 1987;51:1173-1179.
doi: 10.2136/SSSAJ1987.03615995005100050015X
35. Zhang F, Chen X, Vitousek P. An experiment for the world. *Nature*. 2013;497:33-35.
doi: 10.1038/497033a
36. Haring T, Schröder B. A review of model-error in digital soil mapping: Confronting statistical soil landscape models with large-scale field validation data. *Geoderma*. 2016;269:19-29.
37. Aggarwal R, Tewari AK, Srivastava KD, Singh DV. Role of antibiosis in the biological control of spot blotch (*Cochliobolus sativus*) of wheat by *Chaetomium globosum*. *Mycopathologia*. 2004;157(4):369-377.
doi: 10.1023/B: MYCO.0000030446.86370.14
38. Baisden WT, Amundson R, Brenner DL, Cook AC, Kendall C, Harden JW. A multiisotope C and N modeling analysis of soil organic matter turnover and transport as a function of soil depth in a California annual grassland soil chronosequence. *Glob Biogeochem Cycles*. 2002;16:82-1-82-26.
doi: 10.1029/2001GB001823
39. Ma L, Velthof GL, Wang FH, *et al*. Nitrogen and phosphorus use efficiencies and losses in the food chain in China at regional scales in 1980 and 2005. *Sci Total Environ*. 2012;434:51-61.
doi: 10.1016/j.scitotenv.2012.03.028
40. Vanselow AP. Equilibria of the base-exchange reactions of bentonites, permutites, soil colloids, and zeolites. *Soil Sci*. 1932;33:95-114.
doi: 10.1097/00010694-193202000-00002
41. De Boer W, Kowalchuk GA. Nitrification in acid soils: Micro-organisms and mechanisms. *Soil Biol Biochem*. 2001;33:853-866.
doi: 10.1016/S0038-0717(00)00247-9
42. Bolan NS, Adriano DC, Curtin D. Soil acidification and liming interactions with nutrient and heavy metal transformation and bioavailability. *Adv Agron*. 2003;78:215-272.
doi: 10.1016/S0065-2113(02)78006-1
43. Giambalvo D, Ruisi P, Di Miceli G, Frenda AS, Amato G. Nitrogen use efficiency and nitrogen fertilizer recovery of durum wheat genotypes as affected by interspecific competition. *Agron J*. 2010;102:707-715.
doi: 10.2134/agronj2009.0380
44. Lal R. Digging deeper: A holistic perspective of factors affecting soil organic carbon sequestration in agroecosystems. *Glob Change Biol*. 2018;24:3285-3301.
doi: 10.1111/gcb.14054
45. Steven Are K, Adelana AO, Fademi IO, Aina OA. Improving physical properties of degraded soil: Potential of poultry manure and biochar. *Agric Nat Resour*. 2018;51(6):454-462.
doi: 10.1016/j.anres.2018.03.009
46. Chen X, Cui Z, Fan M, *et al.* Producing more grain with lower environmental costs. *Nature*. 2014;514:486-489.
doi: 10.1038/nature13609
47. Liu X, Vitousek PM, Chang Y, Zhang W, Matson P, Zhang F. Evidence for a historic change occurring in China. *Science*. 2016;352:427-428.
doi: 10.1021/acs.est.5b05972
48. Zhang X, Davidson EA, Mauzerall DL, Searchinger TD, Dumas P, Shen Y. Managing nitrogen for sustainable development. *Nature*. 2015;528:51-59.
doi: 10.1038/nature15743
49. Powlson DS, Whitmore AP, Goulding KWT. Soil management in relation to sustainable agriculture and ecosystem services. *Food Policy*. 2011;36:S72-S87.
50. West TO, Post WM. Soil organic carbon sequestration rates by tillage and crop rotation. *Soil Sci Soc Am J*. 2002;66:1930-1946.
doi: 10.2136/sssaj2002.1930
51. Goulding KWT. Soil acidification and the importance of liming agricultural soils with particular reference to the United Kingdom. *Soil Use Manag*. 2016;32:390-399.
doi: 10.1111/sum.12270
52. Bouman BAM, Humphreys E, Tuong TP, Barker R. *Water Management in Irrigated Rice: Coping with Water Scarcity*. Los Baños: The International Rice Research Institute; 2007.
53. Pretty J, Benton TG, Bharucha ZP, *et al.* Global assessment of agricultural system redesign for sustainable intensification. *Nat Sustain*. 2018;1:441-446.
doi: 10.1038/s41893-018-0114-0